Oncology
and Radiotherapy ©
1 (52) 2020: 001-010 • RESEARCH ARTICLE

Detection of brain tumour in 2D MRI: implementation and critical review of clustering-based image segmentation methods

Lim Jia Qi, Norma Alias, Farhana Johar

Department of Mathematical Sciences, 81310 UTM Johor Bahru, Johor, Malaysia

SUMMARY

Image segmentation can be defined as segregation or partitioning of images into multiple regions with the same predefined homogeneity criterion. Image segmentation is a crucial process in medical image analysis. This paper explores and investigates several unsupervised image segmentation approaches and their viability and performances in delineating tumour region in contrast enhanced T1-weighted brain MRI (Magnetic Resonance Imaging) scans. First and foremost, raw CE T1-weighted brain MR images are downloaded from a free online database. The images are then pre-processed and undergo an important process called skull stripping. Then, image segmentation techniques such as k-means clustering, Gaussian mixture model segmentation and fuzzy c-means are applied to the pre-processed MR images. The image segmentation results are evaluated using several performance measures, such as precision, recall, Tanimoto coefficient and Dice similarity index in reference to ground truth images. The highest average Dice coefficient is achieved by k- means (0.189) before post-processing and GMM (0.208) after post-processing. Unsupervised clustering-based brain tumour segmentation based on just image pixel intensity in single-spectral brain MRI without adaptive post-processing algorithm cannot achieve efficient and robust segmentation results.

Key words: image segmentation, brain MR images, fuzzy c-means, k-means clustering, GMM segmentation

Address for correspondence:

Lim Jia Qi, Department of Mathematical Sciences, Faculty of Science, 81310 UTM Johor Bahru, Johor, Malaysia, email: ykj10@hotmail.com

Word count: 6660 **Tables:** 11 **Figures:** 09 **References:** 62

Received: - 23 March, 2020

Accepted: - 10 April, 2020

Published: - 20 April, 2020

INTRODUCTION

Human brain possess a very complex structure, and is the central part of the nervous system. Being one of the most important organ in the human body, the presence of brain tumours, be it benign or malignant can be devastating. Brain cancer is rather rare, consisting of merely 1.95% of all cancers in Malaysia [1, 2]. Nonetheless, brain cancer is highly fatal. As a matter of fact, the five year relative survival rate is only 34.9% according to the report of Central Brain Tumour Registry of the United States (CBTRUS). In view of the severity of brain tumour and lack of effective treatment, early diagnosis of the disease can be crucial for the patient recovery and treatment planning for the doctor. Advanced imaging protocols, like Computed Tomography (CT), Positron Emission Tomography (PET), and MRI have provided unprecedented high resolution of medical images that make medical image analysis possible. In this paper, MRI will be the modality of choice because : 1) MRI is non-invasive, 2) produces multiple slices of images of the same tissue region with different contrast by applying different image acquisition protocols and parameters [3], 3) high contrast of soft tissues and high spatial resolution. In this paper, only contrast enhanced T1-weighted MR image will be considered as multi- spectral MR images analysis is expensive and increases odds of segmentation errors due to inconsistency and misalignment [4].

One of the most important steps in brain tumour characterization, detection and visualization is to perform image segmentation to localize the tumour region. Image segmentation is an image processing technique in which several mutually exclusive regions of interests are isolated and segregated based on predefined criteria depending on the algorithm used [5]. According to Gordillo et al. [6], segmentation of brain tumours can be divided into 3 pathways: manual, semi- automatic and fully automatic. Currently, manual segmentation is often the choice, but the drawbacks are that it is time consuming and heavily relies on the expertise and experience of trained anatomists. This is followed by biopsy (extraction of brain tissue) in conventional clinical trial. One of the primary reason that manual segmentation is still popular is that automated segmentation of brain tumour in medical images can be extremely difficult especially when it comes to delineating "abnormal tissue". Tumour are often non-rigid and complex in shape, vary in size and position and displays huge variability among patients

[6]. Furthermore, intensity homogeneity between surrounding normal tissue and brain tumour and partial volume effect can create confusion within the segmentation algorithm and even radiologists. On the other hand, semi-automated approaches require user input and intervention, which may subject to variability in segmentation results, Even though identification and segmentation of brain tumour in MRI is a great challenge, it is very important in clinical practice for cancer treatment planning and oncology research as a whole. For instance, MRI segmentation can utilized in delineating lesions, image-guided intervention and surgical planning [7]. Owing to high demand and paramount importance of precise image segmentation, various segmentation algorithms with different degree of complexity, either semiautomatic or fully automatic has been put forward.

According to survey done by Despotovi et al., [7], image segmentation of brain MR images can be categorized into: threshold-based, region-based, pixel classification and clustering, atlas-based, model-based and hybrid method. Lately, deep learning has emerged as a popular method in segmentation of brain tumour [8]. Thresholding is a simple image segmentation approach, in which specific intensity value(s), called threshold is determined to separate pixels into their desired class [9] Proposed segmentation of brain tissues into White Matter (WM), Gray Matter (GM), and Cerebrospinal Fluid (CSF) using thresholding and seed region growing technique. Otsu multi-thresholding segmentation with morphological operations on MR images was proposed by Chaddad [10]. Bahadure et al., applied Berkeley Wavelet Transform (BWT) based brain tumour segmentation. An average of 0.82 dice similarity index was reported. Region growing refers to image segmentation process that extract groups of neighbouring connected pixels with similar intensity and fulfil predefined homogeneity criteria [11, 12]. Salman [13] applied a modified version of the traditional region growing method or called modified region growing method in 3D brain MR images containing tumours. More accurate boundary detection after segmentation was reported. Seeded region growing was utilized for image segmentation on both 2D and 3D brain MR images in the work of Weglinski et al., and Shantha kumar, et al., [14, 15] performed region growing segmentation with automated seed point selection by taking account of tumour region features. Similarity index and overlap fraction of 0.817 was reported. Pixel classification and clustering is another type of segmentation method. Under this category, each pixel is treated as an instance or observation and they will be grouped/ clustered in classes either based on trained classification models or some similarity criterion. Juang et al., [16] put forward colour converted segmentation with k-means clustering technique. The gray level of brain MR images was converted into a colour space image and regions in image are labelled by cluster index. Ji et al., [17] proposed a Generalized Rough Fuzzy C-Means Method (GRFCM) for brain MR segmentation. Each cluster is characterized by 3 automatically determined rough fuzzy regions. Each region is balanced by a weighting parameter and the bias field is modelled by linear combination of orthogonal polynomials. The proposed algorithm is more robust and produce more accurate segmentation compared to rough c-means and hybrid clustering algorithms. A segmentation algorithm consisting of Self-Organizing Map (SOM) coupled with learning Vector Quantization (LVQ) was proposed by Demirhan et al., [18]. Multi-spectral MR images from 20 subjects was collected. Average dice similarity indices are 61% for tumour and 77% for edema. Atlas based method can a powerful segmentation method if template of human brain for a population of interest is present. This database can provide information on the brain anatomy and serve as references while segmenting new images. Bauer et al., [19] performed atlas-based segmentation of brain tumour images. A total of 5 patient dataset was investigated and an average of 0.96 dice similarity index for tumour was obtained. For model-based segmentation technique, a continuous model is constructed through understanding of prior knowledge about the object of interest, such as size, location and orientation. They proposed a deformable model, called the Charged Fluid Model (CFM) for segmentation of medical images, such as CT and MRI scans [20]. Poisson's equation was used to guide the evolution of the mathematical model. The main idea of the hybrid approach is to integrate different complementary methods to improve segmentation accuracy. They proposed 2 hybrid segmentation techniques, HASA and EHASA. Both techniques are based on symmetry. The proposed techniques can identify and detect multiple tumours [21]. These techniques do not require any user interaction and are fully automatic. One limitation is that it will not give good results if the tumour is present on the symmetry line. He presented a method for 3D medical image segmentation by combining clustering and classification algorithms [22]. TOP-LBP features and gray level co-occurrence matrix are extracted and random forest is used for classification and segmentation of the necrosis, edema, non-enhanced tumour and enhanced tumour. The dice similarity index for tumour obtained was 0.96 ± 0.01.

Recently, deep learning has quickly emerged as state-of-the-art in biomedical image segmentation due to its superior accuracy, sometimes outperforming clinical experts. However, the biggest bottlenecks for the application of deep learning is the lack of annotated and labelled images [23]. To summarize, although there are wide variety of image segmentation algorithms in the literature, brain tumour segmentation remains a challenging task, due to diverse image content, occlusion, image noise and interference [24]. In view of this, the primary motivation of this study is to assess and compare the performances of several clustering based image segmentation approaches like k-means clustering, Gaussian Mixture Model (GMM) segmentation and fuzzy C-means clustering in terms of execution time and segmentation accuracy (precision, recall, Jaccard index, Dice similarity coefficient). Clustering-based segmentation approaches are unsupervised, which means that the image segmentation techniques do not take class information into consideration. Unsupervised methods are receiving narrow research effort due to difficulty in the integration of prior anatomic knowledge and algorithm [6]. This study aims to bridge the gap by investigating the scalability and practicability of these image segmentation techniques in delineating tumour region in large number of real brain MR images. Lastly, we proposed some modifications to the segmentation algorithms to adapt to brain tumour segmentation and simultaneously minimize parameters adjustment and feedback response (human intervention).

MATERIALS AND METHODS

Figure 1 shows the flow diagram of the overall processes in this research. The details of the implementation of algorithms involved will also be discussed. All the processes in this research are performed in MATLAB 2017a platform using processor Intel(R) Xeon(R) CPU with 32.0 GB RAM.

Data acquisition

A total of 3064 slices of T1-weighted contrast enhanced MR images from 233 patients was downloaded from https://figshare.com/articles/brain_tumour_dataset/1512427. There are three kinds of brain tumour in the MR images downloaded, namely meningioma (708 slices), glioma (1426 slices), and pituitary tumour (930 slices). The brain T1-weighed CE-MRI dataset was acquired from Nanfang Hospital, Guangzhou, China, and General Hospital, Tianjing Medical University, China, from year 2005 to 2010. The images pixel size are of 0.49 × 0.49 mm^2. The slice thickness is 6 mm and the slice gap is 1 mm [25, 26]. Furthermore, the brain tumour in the images has been delineated or segmented by radiologists which can be ground truth images in evaluating and validating the subsequent image segmentation performance. One of the raw brain MR images and its corresponding gray level histogram is shown in Figure 2.

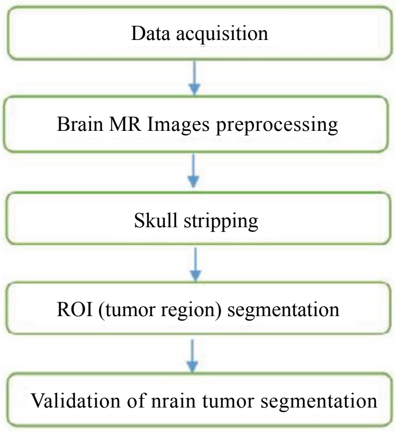

Fig. 1. Flow diagram of research framework

Brain MR images pre-processing

Medical images are often come with poor contrast and corrupted by noises arise from old MRI machine, image transmission and image digitization [15], extracranial tissue and etc. These factors degrade image quality and inevitably affect subsequent segmentation results regardless of methods employed [18]. In view of the above issues, brain MR images pre-processing is a vital step to remove the unwanted interferences present in raw MR images.

There has been numerous image pre-processing methods proposed for the application in MRI in the literature. Some of them includes median filter [27], Gaussian filter, anisotropic filtering [15], contrast enhancement [11], bias field removal, histogram matching [28, 29] and skull stripping [30], The justification behind pre-processing of images is to increase signal to noise ratio, enhance visual appearance for both human and machine vision, remove unnecessary parts in the background and preserving important edges and borders and so on. Several pre-processing techniques will be applied in this research. Steps of pre-processing of pathological brain MR images is presented in Figure 2.

Fig. 2. Process flow of brain MR images pre-processing

First stage of MR images pre-processing is bias field estimation and removal. Bias field is commonly recognized as low frequency smooth varying signals which accounts for intensity non-uniformity or shading in an image. This phenomenon is usually caused by radio frequency coil non-uniformity, eddy currents, patient positioning and etc. [31]. Bias field is undesirable as it reduces the high frequency contents such as borders and contours in an image and cause variation in gray level distribution in the same brain tissues. In this research, second order parametric surface fitting method using Levenberg-Marquadt algorithm, in reference to work of Juntu et al., [32] was applied to remove bias field.

Median filter and anisotropic diffusion filter are two primary de-noising methods in brain MR images. Anisotropic diffusion filter are computationally more complex and have several parameters to select to control the operation. Thus, median filter was chosen. A 5 × 5 median filter was applied to eliminate noise and simultaneously retain important borders. Then, histogram stretching or also known as inner cropping was performed on the image. The goal is to increase contrast without modifying shape of the original histogram.

Skull stripping

Essentially, brain MR images contain non-brain tissue, also known as extra-cranial tissues, such as skull, fat, muscle and connective tissues. The existence of these non-cerebral tissue can be a major obstacle for quantitative analysis later on. Thus, elimination of non-brain tissues, or also known as skull stripping is another vital step before the segmentation of brain MR images can be carried out. In fact, skull stripping is the preliminary step before other further image processing such as image registration [33], tissue classification [34], multiple sclerosis analysis [35], and even diagnosis of neurodegenerative disease like Alzheimer's disease [36].

Published review studies from Fennema- Kalavathi et al., and Fennema-Notestine C et al. [30, 37] show that different methodologies have its own advantages and limitations. Even though there is extensive research on skull stripping on brain MRI, majority of the methods do not give satisfactory results over a wide range of scan types due to anatomical variation, imaging artefacts, varying contrast properties and so on [38]. In this study, multi-level thresholding followed by morphology based [10] post-processing method [39] was implemented.

The proposed algorithm consists of 3 phases:

1) Four-class thresholding. The three thresholds, k1, k2 and k3 separating 4 classes are found using thresholding method proposed by Otsu [40]. Otsu thresholding is one of

the binarization algorithms that was popularly employed in separating foreground and background in an image. The threshold selection is based upon the basis of maximizing inter-class variance and minimizing intra-class variance. The pixels that is above $k1$ and less than or equal to $k3$ are believed to be brain region and will be retained for next phase

2) Morphological operations commences with erosion, followed by largest connected component analysis [41], dilation and lastly morphological flood fill operation. The structural elements used is disc shape with radius of 5 units for both erosion as well as dilation operations. Erosion on the binary images is to remove small disconnected regions, while dilation is to smoothen the boundary of object. With the assumption that the brain is the largest connected component in brain MRI [42], connected component processing was performed and the largest connected object (brain) are preserved. Flood fill operation aims at filling small holes in binary image

3) Mask the binary image with the pre-processed image which produces skull stripped image to obtain grayscale brain image. The overall processes of pre-processing and skull stripping are depicted in (Figure 3)

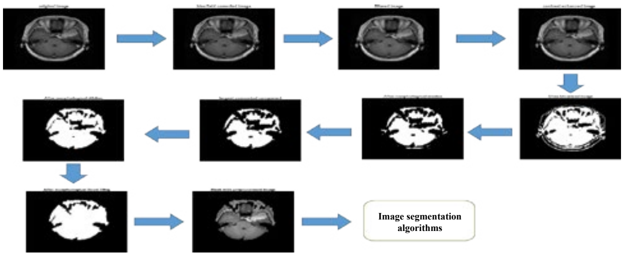

Fig. 3. Workflow of preprocessing and skull stripping

ROI (tumour region) segmentation

In the analysis of brain MRI, image segmentation is frequently used for visualizing brain anatomical structures, such as WM, GM, CSF, and tumour region. In this research, the emphasis will be put on segmenting brain tumour from other brain structures. This will be especially helpful in studying the shapes, location and structures of the tumour. Based on the review of previous works, 4 clusters are often chosen as the parameter [43, 44] although it is believed that the tumour tissues can further divided into active regions, edema and necrotic core [6, 45, 46]. In four clusters setting, the clusters with highest mean pixel intensity will be extracted.

In addition, based on the review on clustering-based techniques in delineating tumour region, the authors also noticed that some works proposed post-processing while others do not. The post-processing found in literature include morphological filtering [44] and largest connected components [47]. In view of this, this study aims to combine these two methods in delineating the final tumour mask. Table 1 shows the values of parameters used in the clustering algorithms.

Tab. 1. Parameters in common for the proposed image segmentation methods

Parameters	Values
K, number of clusters	4
ε, error tolerance	10^{-5}
A_{min}, area threshold in binary tumour mask	30
mi, maximum number of iteration	100

K-means clustering: Clustering, being an unsupervised learning method, can be applied in image segmentation and k-means clustering is one of the most popular clustering method in brain tumour detection [48, 49]. It is simple and can cope with large number of variables [50]. The parameter, k as its name suggests is a user defined parameter that specify the number of clusters, which can be critical factor in final segmentation result. Low k produces small number of groups that segregate gray matter and white matter, whereas high k probably results in over-segmentation (a lot of disconnected regions) that can increase difficulty in post-processing. Therefore, we perform k-means clustering with different k to evaluate the effect of k on the segmentation results.

The pseudo-code of k-means clustering in segmentation of brain tumour from MRI in this research is shown below:

1) Initialize parameter k, maximum number of iterations, i, and error tolerance

2) Randomly generate centroid for each k clusters, while $i < mi$

Calculate the dissimilarity measures (Euclidean distance) between each centroids with other pixels:

$$d_{jk}=\sqrt{(p_j-p^k_{centroid})^2}=\left|p_j-p^k_{centroidk}\right|$$

Determine the shortest distance of each pixel with centroids.

Assign each pixel to a specific class, Cj corresponds to the nearest centroid.

$Cj = \arg\min d\, \frac{j}{k}$

Calculate J, objective function.

$(i) = \frac{1}{mxn} \times \mathrm{d} \times \mathrm{dT}$

Update the cluster centroids by formulae below:

$pk\ centroid = \frac{\Sigma jpj}{nk}$

If $i \geq 2$

If $|(i)\text{-}J(i\text{-}1)| < \varepsilon$

Break while loop.

3) End while

m is the number of row of the image, n is the number of column of the image, is row vector in which each entry represents distance of each data to its centroid.

GMM based segmentation: GMM is another common probabilistic parametric model in brain tumour segmentation [51-53]. Unlike k-means clustering that assigns each pixel to only one label (hard assignment), each pixel is assigned with different probability corresponding to each class specified (soft assignment). Similar to k-means clustering, the number of clusters is arbitrary.

Let xi $A = \pi r^2$ denotes the pixel intensities of images and N be the number of pixels of images. The pseudo-code of GMM based segmentation is shown below:

1) Initialize number of clusters, k and maximum number of iteration, mi

2) Initialize mean, μk of each class as pixel intensities picked

randomly; initialize standard deviation, σk of each class as overall standard deviation; initialize prior probability, φk of each class as $1K$; initialize iteration counter as i=0

3) Run the expectation-maximization algorithm

while i<mi

i=i+1

Calculate probability of each pixel based on Gaussian probability density function (pdf) for each class:

$$p(xi \mid \mu k, \sigma k) = \frac{1}{\sqrt{2\pi\sigma k}} \exp\left(-\frac{(\mathrm{xi}-\mu\mathrm{k})^2}{2\sigma k 2}\right)$$

Calculate the normalized pdf (posterior probability of a certain pixel belonging to class k):

$$z_{ik} = \int \frac{\varphi\mathrm{kp}(\mathrm{xi}|\mu\mathrm{k},\sigma\mathrm{k})}{\sum K = 1\varphi\mathrm{kp}(\mathrm{xi}|\mu\mathrm{k},\sigma\mathrm{k})}$$

$\mu old \leftarrow \mu$

For each cluster, k, update mean, standard deviation and prior probability:

$$\varphi k = \frac{\sum i = 1\mathrm{zik}}{N}$$

$$\mu k = \frac{\sum \frac{N}{I=1} ZikXi}{\sum \frac{N}{i=1} zik}$$

$$\sigma k = \frac{\sum \frac{N}{i=1} Zik(Xi-\mu k)(Xi-\mu k)T}{\sum \frac{N}{i=1} Zik}$$

Calculate J, log-likelihood function

$$J(i) = \frac{1}{N} \sum_{i=1}^{N} log \sum_{k=1}^{k} \varphi\mathrm{kp}_{\mathrm{ik}}(\mathrm{xi}|\mu\mathrm{k}, \sigma\mathrm{k})$$

If i≥2

If |(i)-J(i-1)|<ε

Break while loop

4) End if

Fuzzy C-means: Fuzzy c-means algorithm has been widely applied in image segmentation since it was proposed by Bezdek et al., [54]. The algorithm works by assigning membership to each data points (pixels) according to distance of the data to each cluster centers (centroids). Soft assignment of membership is based on fuzzy logic which gives fuzzy values to any particular pixels to be lying in either of the clusters.

1) Initialize number of clusters, K and maximum number of iteration, mi.

2) Randomly initialize membership matrix, U_{ik}, where i denotes the sample indices and k is the cluster indices with the condition U_{ik}∈[0,1] and $\sum_{k=1}^{K} Uk = 1$. Initialize fuzzifier, m=2 in reference to work of Bezdek and Pal [54, 55] which suggest the use of value in the interval [1.5, 2.5]

Let l=0

while l<mi

l=i+1

Calculate the cluster centroids, ak as follows:

$$a_{\mathrm{k}} = \frac{\sum_{i=1}^{n} \mu \frac{m}{ik}}{\sum_{i=1}^{n} \mu \frac{m}{ik}} .xi$$

Update U_{ik} by the following formula:

$$\mu \frac{l}{ik} = \frac{1}{\sum_{i=1}^{n} \frac{\| \mathrm{x}_i - \mathrm{a}_j \| 2}{\| \mathrm{x}_i - \mathrm{a}_k \| m-1}}$$

If l≥2

If $\| Uikl - Uikl-1 \| < \varepsilon$

Break while loop, End if End while.

Post processing: Post processing is conducted to obtain the exact location of tumour region without the assistance of human experts. First, the cluster corresponding to highest mean pixel intensity will be chosen and region with area less than 30 pixels will be eliminated. Next, there are primarily two main steps: morphological opening followed by largest connected component analysis. Morphological opening is performed with disk structuring element of radius 10 to remove small objects and retain the shape and size of bigger objects; largest connected component is assumed to be the tumour region.

Performance evaluation of each image segmentation approaches: Objective and accurate assessment of different image segmentation algorithms on a specific types of image is crucial in helping researchers to properly adjust parameters in each algorithms, get a better picture of strengths and weaknesses

Tab. 2. Performance measures and their respective formula and details

Performance measures	Formula	Details
Execution time (s)	-	Quantify the speed of algorithms proposed.
Precision	$Precision = \frac{n(A \cap B)}{n(A)}$	Proportion of machine generated positive pixels overlap with ground truth positive pixels.
Recall	$Recall = \frac{n(A \cap B)}{n(A)}$	Proportion of ground truth positive pixels correctly identified by image segmentation algorithms.
Jaccard similarity coefficient	$Jaccard\ coefficient, J = \frac{n(A \cap B)}{n(A \cap B)}$	Measure of similarity between two binary tumour masks from both segmented and ground truth.
Dice similarity coefficient	$Dice\ coefficient, D= D = \frac{2 \times n(A \cap B)}{n(A) + n(B)}$	Measure of similarity between two binary tumour masks from both segmented and ground truth.

and select the best methods. In this study, we will employ empirical discrepancy methods in evaluating the goodness of segmentation results due to availability of gold standard or ground truth binary tumour mask [56]. Widely accepted metric like execution time, precision, recall [57], Jaccard coefficient, and Dice similarity coefficient are used. Let *A* and *B* denote the sets of positive pixels (pixels labelled as tumour) by the ground truth and image segmentation methods respectively. (*A*) denotes the number of elements present in set *A*. The details of each performance measures are listed in Table 2.

RESULTS

In this section, performances of the proposed semi-automatic clustering-based image segmentation algorithms in delineating tumour region will be evaluated based on the ground truth provided alongside the repository. We intend to understand the consistency of the proposed method in large number of 2D single spectral (e.g. in this study, CE T1-weighted MRI) MR images. Section 3.1 discuss the performance of image segmentation without post-processing; section 3.2 discuss the performance of image segmentation with post-processing.

Performance of image segmentation methods without post-processing

As shown in Table 3, the average run time of image segmentation methods can be arranged in ascending order such that: k-means, GMM followed by FCM. This demonstrates the superiority of k-means clustering in terms of computational efficiency.

K-means clustering has the highest precision, Jaccard index and Dice coefficient in comparison to GMM and FCM clustering method. Based on the high standard deviation observed in Tables 4-7 and presence of abundant outliers in Figures 4-8 across all image segmentation approaches, the accuracy in the segmentation results of the proposed methods is inconsistent, suggesting the inability of unsupervised clustering methods in adapting to different MR scans.

Performance of image segmentation methods with post-processing

K-means clustering achieves the highest average precision

Tab. 3. Average execution time of each image segmentation methods

Parameter	Average runtime (s)
k-means	0.071
GMM	2.338
FCM	11.264

Tab. 4. Statistical measures of precision of each image segmentation methods (without post-processing)

Image Segmentation Methods	k-means	GMM	FCM
Min	0.000	0.000	0.000
First Quartile	0.011	0.011	0.014
Median	0.082	0.078	0.031
Third Quartile	0.231	0.222	0.065
Max	1.000	1.000	0.313
Mean	0.165	0.159	0.045
Standard Deviation	0.214	0.208	0.042

Tab. 5. Statistical measures of recall of each image segmentation methods (without post-processing)

Image Segmentation Methods	k-means	GMM	FCM
Min	0.000	0.000	0.000
First Quartile	0.025	0.022	0.957
Median	0.273	0.267	0.998
Third Quartile	0.665	0.710	1.000
Max	0.991	0.996	1.000
Mean	0.352	0.366	0.889
Standard Deviation	0.326	0.343	0.255

Tab. 6. Statistical measures of Jaccard index of each image segmentation methods (without post-processing)

Image Segmentation Methods	k-means	GMM	FCM
Min	0.000	0.000	0.000
First quartile	0.008	0.007	0.014
median	0.060	0.056	0.031
Third quartile	0.179	0.166	0.065
Max	0.898	0.931	0.313
Mean	0.123	0.115	0.045
Standard deviation	0.157	0.149	0.042

Tab. 7. Statistical measures of Dice similarity index of each image segmentation methods (without post- processing)

Image Segmentation Methods	k-means	GMM	FCM
Min	0.000	0.000	0.000
First Quartile	0.015	0.014	0.027
Median	0.114	0.106	0.060
Third Quartile	0.304	0.285	0.122
Max	0.946	0.964	0.477
Mean	0.189	0.179	0.083
Standard Deviation	0.209	0.201	0.073

Tab. 8. Statistical measures of precision of each image segmentation methods (after post-processing)

Image Segmentation Methods	k-means	GMM	FCM
Min	0.000	0.000	0.000
First Quartile	0.000	0.000	0.014
Median	0.000	0.000	0.035
Third Quartile	0.970	0.953	0.073
Max	1.000	1.000	0.947
Mean	**0.300**	0.292	0.050
Standard Deviation	0.451	0.446	0.051

Tab. 9. Statistical measures of recall of each image segmentation methods (after post-processing)

Image Segmentation Methods	k-means	GMM	FCM
Min	0.000	0.000	0.000
First Quartile	0.000	0.000	0.968
Median	0.000	0.000	1.000
Third Quartile	0.241	0.248	1.000
Max	0.986	1.000	1.000
Mean	0.167	0.179	0.855
Standard Deviation	0.290	0.312	0.317

Tab. 10. Statistical measures of Jaccard index of each image segmentation methods (after post-processing)

Image Segmentation Methods	k-means	GMM	FCM
Min	0.000	0.000	0.000
First Quartile	0.000	0.000	0.014
Median	0.000	0.000	0.035
Third Quartile	0.231	0.241	0.073
Max	0.956	0.962	0.941
Mean	0.163	0.173	0.050
Standard Deviation	0.283	0.302	0.051

Tab. 11. Statistical measures of Dice similarity index of each image segmentation methods (after post-processing)

Image Segmentation Methods	k-means	GMM	FCM
Min	0.000	0.000	0.000
First Quartile	0.000	0.000	0.028
Median	0.000	0.000	0.067
Third Quartile	0.375	0.389	0.136
Max	0.977	0.980	0.969
Mean	0.200	**0.208**	0.092
Standard Deviation	0.330	0.345	0.084

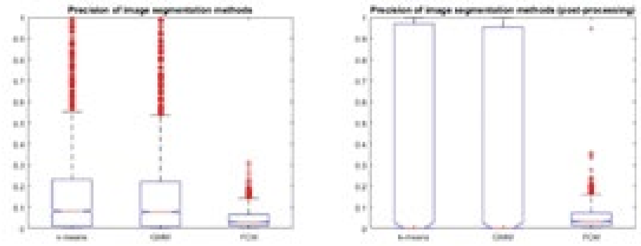

Fig. 4. Box-plot for distribution of precision before and after post-processing

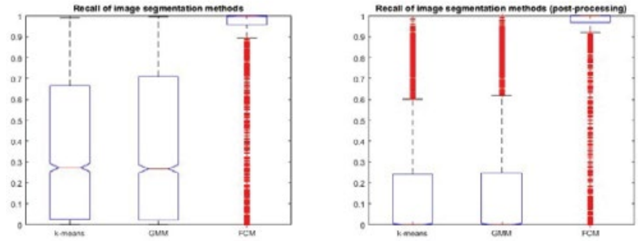

Fig. 5. Box-plot for distribution of recall before and after post-processing

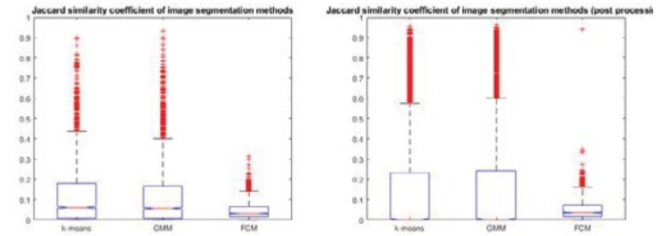

Fig. 6. Box-plot for distribution of Jaccard index before and after post-processing

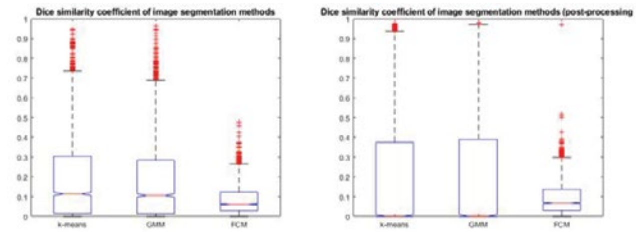

Fig. 7. Box-plot for distribution of Dice similarity index before and after post-processing

DISCUSSION

In summary, the performance of all the clustering-based brain tumour segmentation is highly inconsistent, manifested by the high standard deviation observed in performance measures. This clearly shows that by using image pixel intensity in single spectral MRI alone as features is insufficient in accurately predicting tumour region. Prior knowledge on tumour location and shape should be exploited. It is noted that FCM algorithm suffers from long computational time, has the lowest precision, Dice and Jaccard similarity indices. This finding contradicts to some results reported in literature [58, 59].

We would argue this discrepancy arise due to the use of different MRI modality. In our case, contrast enhanced T1-weighted data normally has larger pixel intensity differences between tumour and surrounding tissues (in other words higher contrast to noise ratio [60] while other images might be affected by partial volume effect (homogeneity between tumour and normal tissues), thus fuzzy assigning of pixels to each cluster may be more efficient in that case. The unusual high recall and low precision indicate that FCM tends to overestimate tumour area as shown in Figure 8.

Fig. 8. (Left) Tumour region segmented by FCM; (Right) ground truth tumour region

Plenty of previous works regarding the brain tumour segmentation of 2D MR images share these similarities: 1) low number of images, 2) lack of gold standard, thus no empirical results (e.g. Dice, Jaccard) can be reported. It is also noticed that some researches do not include skull stripping and post-processing before and after image segmentation algorithms, which can be critical for accurate and efficient brain tumour segmentation. This study bridges the gap by implementing automatic unsupervised clustering algorithm on large amount (3064 slices) of 2D MR images with ground truth, offering clearer insight on the generalizability of clustering methods, in segmentation of brain tumour.

Lastly, the reasons behind the poor performance of the proposed algorithms as compared to what reported in the literature:

1) Lack of shape or intensity priors on the tumours [61]. As such, clustering algorithm based solely on pixel intensity is unable detect the exact tumour region that can vary in shapes and location

2) The unsupervised clustering algorithms proposed in the literature normally exploit anatomic objective measures and include interactive post-processing while our study do not exploit any prior assumptions and implement automatic post-processing

3) Our method cannot detect necrotic core, normally displayed as hypointense region [62]

4) Skull stripping methods proposed may accidentally remove tumour tissues, especially those that share similar intensity with non-brain tissues as shown in Figure 9.

5) The proposed post-processing method is unable to capture ROI accurately across all MR images

Fig. 9. (Left) Skull stripped images; (Right) ground truth tumour region

CONCLUSION

In this paper, we presented several clustering-based brain tumour segmentation using CE T1-weighted MR images. A few common evaluation measures based on manually delineated tumour region are utilized to validate the segmentation performances of each method. Results show that the introduced k-means and GMM is more accurate before and after post-processing. The average dice similarity of k-means (before post-processing: 0.189; after post-processing: 0.2), while for GMM (before post-processing: 0.179; after post-processing: 0.208). Additionally, the segmentation accuracy of this image segmentation approaches can vary greatly among all the 3064 datasets analyzed, based on the high standard deviation in performance metrics. All in all, unsupervised clustering-based brain tumour segmentation with the use of solely image pixel intensity in single-spectral brain MRI without adaptive post-processing algorithm cannot achieve efficient and robust segmentation results.

In view of these limitations of the proposed methods, future research should be oriented towards utilizing more image features like using co-registered multi-spectral MRI features and spatial information (super-pixel segmentation). Sophisticated image segmentation methods like deep learning can be another alternative to enhance the brain tumour segmentation accuracy.

FUNDINGS

A special thanks to Universiti Teknologi Malaysia (UTM) for the opportunity to carry out the research and Ministry of Education (MOE) for financial support. This project was supported by Research University Grant [Vot Number: 19H03] initiated by UTM and MOE.

REFERENCES

1. Bondy ML, Scheurer ME, Malmer B, Barnholtz-Sloan JS, Davis FG, et al. Brain tumor epidemiology: consensus from the brain tumor epidemiology consortium. Cancer. 2008;113:1953-1968.
2. CC Lim, G Yahaya, Lim T. Second report of the national cancer registry. Cancer Incidence in Malaysia. 2003.
3. Mortazavi D, Kouzani AZ, Soltanian-Zadeh H. Segmentation of multiple sclerosis lesions in MR images: a review. Neuroradiol. 2012;54:299-320.
4. Nabizadeh N, Kubat M. Brain tumors detection and segmentation in MR images: Gabor wavelet vs. statistical features. Comput Electr Eng. 2015;45:286-301.
5. Vishnuvarthanan G, Rajasekaran MP, Subbaraj P, Vishnuvarthanan A. An unsupervised learning method with a clustering approach for tumor identification and tissue segmentation in magnetic resonance brain images. Applied Soft Comput. 2016;38:190-212.
6. Gordillo N, Montseny E, Sobrevilla P. State of the art survey on MRI brain tumor segmentation. Magn Reson Imaging. 2013;31:1426-1438.
7. Despotovi I, Goossens B, Philips W. MRI segmentation of the human brain: Challenges, Methods, and Applications. Comput Math Method M. 2015;2015:1-23.
8. Havaei A, Warde-Farley D, Biard A, Courville A, Bengio Y, et al. Brain tumor segmentation with deep neural networks. Med Image Anal. 2017;35:18-31.
9. Shanthi KJ, Kumar MS. Skull stripping and automatic segmentation of brain MRI using seed growth and threshold techniques. Paper presented at the 2007 International Conference on Intelligent and Advanced Systems. 2007.
10. Chaddad A. Automated feature extraction in brain tumor by magnetic resonance imaging using gaussian mixture models. Intern J Biomed Imaging. 2015;2015:1-11.
11. Bahadure NB, Ray AK, Thethi HP. Image analysis for MRI based brain tumor detection and feature extraction using biologically inspired BWT and SVM. Intern J Biomed Imaging. 2017;2017:1-12.
12. Wong KP. Medical image segmentation: methods and applications in functional imaging. Handbook of Biomedical Image Analysis: 2005;2:111-182.
13. Salman YM. Modified technique for volumetric brain tumor measurements. J Biomedi Sci Eng. 2009;2:16-19.
14. Węgliński T, Fabijańska A. Brain tumor segmentation from MRI data sets using region growing approach. Paper presented at the Perspective Technologies and Methods in MEMS Design. 2011.
15. Shantha kumar P, Ganeshkumar P. Performance analysis of classifier for brain tumor detection and diagnosis. Comput Electrical Eng. 2015;45:302-311.
16. Juang LH, Wu MN. MRI Brain lesion image detection based on color-converted K-means clustering segmentation. Measurement. 2010;43:941-949.
17. Ji Z, Sun Q, Xia Y, Chen Q, Xia D, et al. Generalized rough fuzzy c-means algorithm for brain MR image segmentation. Comput Methods Programs Biomed. 2012;108:644-655.
18. Demirhan A, Toru M, Guler I. Segmentation of tumor and edema along with healthy tissues of brain using wavelets and neural networks. IEEE J Biomed Health Inform. 2015;19:1451-1458.
19. Bauer S, Seiler C, Bardyn T, Buechler P, Reyes M. Atlas- based segmentation of brain tumor images using a Markov Random Field-based tumor growth model and non-rigid registration. Annual International Conference of the IEEE Engineering in Medicine and Biology. 2010.
20. Chang HH, Valentino DJ. An electrostatic deformable model for medical image segmentation. Comput Med Imaging Graph. 2008;32:22-35.
21. Saddique M, Kazmi JH, Qureshi K. A hybrid approach of using symmetry technique for brain tumor segmentation. Comput Math Methods Med. 2014:10.
22. Abbasi S, Pour FT. A hybrid approach for detection of brain tumor in MRI images. 21th Iranian Conference on Biomedical Engineering (ICBME). 2014.
23. Litjens G, Kooi T, Bejnordi BE, Setio AA, Ciompi F, et al. A survey on deep learning in medical image analysis. Med Image Anal. 2017;42:60-88.
24. Abdel-Maksoud E, Elmogy M, Al-Awadi R. Brain tumor segmentation based on a hybrid clustering technique. Egyptian Inform J. 2015;16:71-81.
25. Cheng J, Huang W, Cao S, Yang R, Yang W, et al. Enhanced performance of brain tumor classification via tumor region augmentation and partition. PLoS One. 2015;10:e0140381.
26. Cheng J, Yang W, Huang M, Huang W, Jiang J, et al. Retrieval of brain tumors by adaptive spatial pooling and fisher vector representation. PLoS One. 2016;1;e0157112.
27. Alfonse M, Abdel-Badeeh M. An automatic classification of brain tumors through MRI using support vector machine. Egyptian Comput Sci J. 2016;140:11-21.
28. Li C, Gore JC, Davatzikos C. Multiplicative intrinsic component optimization (MICO) for MRI bias field estimation and tissue segmentation. Magnet Reson Imaging. 2014;32:913-923.
29. Zacharaki EI, Kanas VG, Davatzikos C. Investigating machine learning techniques for MRI-based classification of brain neoplasms. Int J Comput Assist Radiol Surg. 2011;6:821-828.
30. Kalavathi P, Prasath VBS. Methods on skull stripping of MRI head scan images-a review. J Digit Imaging. 2016;29:365-379.
31. Likar B, Viergever MA, Pernus F. Retrospective correction of MR intensity inhomogeneity by information minimization. IEEE Transactions on Med Imaging, 2001;20:1398-1410.
32. Juntu J, Sijbers J, Van Dyck D, Gielen, J. Bias Field Correction for MRI Images. Paper presented at the Computer Recognition Systems. 2005.
33. Dinggang S, Davatzikos C. HAMMER: hierarchical attribute matching mechanism for elastic registration. IEEE Transactions on Med Imaging. 2002;21;1421-1439.

34. Wang L, ChenY, Pan X, Hong X, Xia, D. Level set segmentation of brain magnetic resonance images based on local Gaussian distribution fitting energy. J Neurosci Methods. 2010;188;316-325.

35. Sharma J, Sanfilipo MP, Benedict RH, Weinstock-Guttman B, Munschauer FE. Whole-brain atrophy in multiple sclerosis measured by automated versus semiautomated MR imaging segmentation. AJNR Am J Neuroradiol. 2004;25:985-996.

36. Rusinek H, De Leon MJ, George AE, Stylopoulos LA, Chandra R, et al. Alzheimer disease: measuring loss of cerebral gray matter with MR imaging. Radiol. 1991;178:109-114.

37. Fennema-Notestine C, Ozyurt IB, Clark CP, Morris S, Bischoff-Grethe A, et al. Quantitative evaluation of automated skull-stripping methods applied to contemporary and legacy images: effects of diagnosis, bias correction, and slice location. Human Brain Mapping. 2006;27:99-113.

38. Park JG, Lee C. Skull stripping based on region growing for magnetic resonance brain images. Neuroimage. 2009;47:1394-1407.

39. Swiebocka-Wiek J. Skull stripping for mri images using morphological operators. Paper presented at the computer information systems and industrial management, Cham. 2016

40. Otsu N. A threshold selection method from gray-level histograms. IEEE Transactions on Systems, Man, and Cybernetics. 1979;9:62-66.

41. Yazdani S, Yusof R, Karimian A, Mitsukira Y, Hematian A. Automatic region-based brain classification of mri-t1 data. PLoS One. 2016;611:e0151326.

42. Shan ZY, Yue GH, Liu JZ. Automated histogram-based brain segmentation in t1-weighted three-dimensional magnetic resonance head images. Neuroimage. 2002;17:1587-1598.

43. Arakeri MP, Redy R. Efficient fuzzy clustering based approach to brain tumor segmentation on MRI images. Paper presented at the Computational Intelligence and Information Technology, Berlin, Heidelberg. 2011.

44. Joseph R. Brain tumor MRI image segmentation and detection in image processing. Intern J Res Eng Tech. 2014;3:1-5.

45. Jin L, Min L, Wang J, Fangxiang W, Liu T, et al. A survey of MRI-based brain tumor segmentation methods. Tsinghua Sci Tech. 2014;19:578-595.

46. IŞıN A, Direkoğlu C, ŞAH M. Review of MRI-based brain tumor image segmentation using deep learning methods. Procedia Comput Sci. 2016;102:317-324.

47. Oliveira G, Varoto R, Cliquet A. Brain tumor segmentation in magnetic resonance images using genetic algorithm clustering and adaboost classifier. 11th International Joint Conference on Biomedical Engineering Systems and Technologies. 2018;2:77-82

48. Foster KR, Koprowski R, Skufca JD. Machine learning, medical diagnosis, and biomedical engineering research-commentary. Biomed Eng Online. 2014;13:94.

49. Paul TU, Bandhyopadhyay SK. Segmentation of brain tumor from brain MRI images reintroducing k-means with advanced dual localization method. Intern J Eng Res App. 2012;2:226-231.

50. Dhanachandra N, Manglem K, Chanu YJ. Image segmentation using k-means clustering algorithm and subtractive clustering algorithm. Procedia Comput Sci. 2015;54:764-771.

51. Moon N, Bullitt E, Van Leemput K, Gerig G. Automatic brain and tumor segmentation. Paper presented at the medical image computing and computer-assisted intervention-MICCAI, Berlin, Heidelberg. 2002.

52. Baid U, Talbar S, Talbar S. Comparative study of k-means, gaussian mixture model, fuzzy c-means algorithms for brain tumor segmentation. Paper presented at the International Conference on Communication and Signal Processing. 2016.

53. Zhao L, Wu W, Corso JJ. Brain tumor segmentation based on GMM and active contour method with a model-aware edge map. 2012.

54. Bezdek JC, Ehrlich R, Full W. FCM: The fuzzy c-means clustering algorithm. Comput Geosci. 1984;10:191-203.

55. Pal NR, Bezdek JC. On cluster validity for the fuzzy c-means model. IEEE Transactions on Fuzzy Systems. 1995;3:370-379.

56. Zhang YJ. A survey on evaluation methods for image segmentation. Pattern Recog. 1996;29:1335-1346.

57. Pont-Tuset J, Marques F. Supervised evaluation of image segmentation and object proposal techniques. IEEE Transactions on Pattern Analysis and Machine Intelligence. 2016;38:1465-1478.

58. Mansoory MS, Behboudi M, Refahi S. Performance evaluation of mri tumor segmentation using clustering algorithms. Arch Med. 2018;10:11.

59. V Malathy, Kamali SM. Brain tumor segmentation from brain magnetic resonance images using clustering algorithm. Intern J Innovat Tech Explore Eng. 2019;8:625-629.

60. Ross MR, Schomer DF, Chappell P, Enzmann DR. MR imaging of head and neck tumors: comparison of T1-weighted contrast-enhanced fat-suppressed images with conventional T2-weighted and fast spin-echo T2-weighted images. Am J Roentgenol. 1994;163:173-178.

61. Popuri K, Cobzas D, Murtha A, Jägersand M. 3D Variational brain tumor segmentation using Dirichlet priors on a clustered feature set. Int J Comput Assist Radiol Surg. 2012;7:493-506.

62. Militello C, Rundo L, Vitabile S, Russo G, Pisciotta P, et al. Gamma Knife treatment planning: MR brain tumor segmentation and volume measurement based on unsupervised Fuzzy C-Means clustering. Intern J Imaging Sys Techn. 2015;25:213-225.